

The Ising model with a periodic spin-lattice coupling on the triangular lattice

R. M. L. Nascimento,¹ Claudio J. DaSilva,² L. S. Ferreira,¹ and A. A. Caparica¹

¹*Instituto de Física, Universidade Federal de Goiás, Av. Esperança s/n, 74.690-900, Goiânia, GO, Brazil*

²*Instituto Federal de Goiás, Rua 76, Centro, Goiânia - GO, Brazil*

In this work, we study and evaluate the impact of a periodic spin-lattice coupling in an Ising-like system on a 2D triangular lattice. Our proposed simple Hamiltonian considers this additional interaction as an effect of preferential phonon propagation direction augmented by the symmetry of the underline lattice. The simplified analytical description of this new model brought us consistent information about its ground state and thermal behavior, and allowed us to highlight a singularity where the model behaves as several decoupled one-dimensional Ising systems. A thorough analysis was obtained via numerical simulations using the Wang-Landau Monte Carlo method that estimates the density of states $g(E)$ to explore the phase diagram and other thermodynamic properties of interest. Also, we used the finite size scaling technique to characterize the critical exponents and the nature of the phase transitions that, despite the strong influence of the spin-lattice coupling, turned out to be within the same universality class as the original 2D Ising model.

I. INTRODUCTION

The study of magnetic systems is one of the most relevant in condensed matter physics. Since its discovery, several scientific works and technological applications have been developed [1, 2]. They focused on proposing several models based on mathematical expressions capable of describing or at least approaching the observed phenomenon. Such approaches start from microscopic modeling of magnetic moments to the point of reproducing the macroscopic behavior of these phenomena[3].

One of the works of great prominence following this approach is the Ising model developed by Ernest Ising in 1920 [4]. Since then, several seminal studies have emerged to improve the comprehension of the spin interaction process. In this list, we can highlight the Heisenberg model and the XY model [5], as well as the Potts model [6], the J1-J2 model [7, 8], among others.

Although each model has its particular scope, a common factor among them is that they only use spin-spin exchange interactions. However, modeling these types of systems consists of arranging magnetic moments on a crystalline lattice[9], not taking into account the influence of the lattice vibration on the thermal properties of these systems.

Some works investigate what the elastic wave of the crystalline lattice can promote in the dynamics of the spins. One of the first dates back to 1975 [10] where, in addition to other singularities, it was able to present strong indications of the impact that the coupling with the lattice can promote on the critical temperature and the type of phase transition. After this study, other works followed the same approach but allowed greater freedom for the orientation of the spins [11–13]. This whole trajectory up to the present day has made the approach involving the spin interaction and the degrees of freedom of the lattice relevant to the study of electronic materials such as single-layer semiconductors [14], which make up the list of devices with great potential for spintronics [15].

In addition, still based on this methodology, studies that consider the influence of lattice vibration on interactions also contribute to the comprehension of the phenomena involving superconductivity [16], ferroelectricity [17] and other unique characteristics of great interest for the study of magnetic materials. Faced with the immense influence that lattice vibration can exert on magnetic interactions, we feel motivated to propose this work in which we seek to understand how this vibration can interfere with the behavior of Ising-like spin systems.

These studies can become more relevant when we consider the vibration of the crystalline lattice as a whole, i.e., together with its symmetry. Some of the consequences of this proposal culminated in the ability to represent certain models in specific situations and to indicate a more physically acceptable formulation for the description of the observed phenomena. Therefore, the vibration of the crystalline lattice can change the lattice parameters, moving atoms closer or further away. This perspective appears when one is evaluating the impact of phonon dynamics on the behavior of magnetic systems, considering the spin-lattice coupling [18, 19]. In this case, when one couple the spin-exchange interaction and the distances between two magnetic ions, it is possible to obtain a Hamiltonian that describes the interference caused by the phonons to this interaction [20]. In addition, additional energy is also generally proposed that takes into account the elastic energy, which, in its simplest form, only considers the length of bonds or the magnitude of displacements of sites related to bond-phonon models [21] and site-phonon [22], respectively. The first one relies on the fact that each bond vibrates independently, while the other tries to guarantee that each site will have to oscillate independently.

Therefore, the system energy will be directly related to the degrees of freedom of the crystalline lattice via negligible displacements of the equilibrium positions, requiring the construction of continuous models. As a result, this requirement increases the complexity of the calculations and proposed models where, in most cases, simulations require a high computational cost [23–26]. On

the other hand, in our proposal, we want to know the influence of the lattice vibration in an Ising-like triangular lattice model, in which we reduce the degrees of freedom of the spins and neglect the instantaneous positions of the atoms. Consequently, the effect of this lattice vibration goes into the exchange interaction dependent on the interacting sites.

Promptly, assuming a lattice model has the potential to enable the use of entropic simulations to obtain thermodynamic properties, as well as the analysis of the criticality of the model on the influence of lattice vibration.

We start this paper by describing the proposed model in section II. In section III, we address the computational details used to obtain the results. Then, in section IV, we present the thermodynamic properties and discuss the main characteristics of the influence of lattice vibration on the triangular Ising model. Finally, in section V we summarize the results and allude to some final remarks.

II. THE MODEL

The crystalline lattice vibration can change the lattice parameters, making the atoms approach or move away. Such a situation can produce a variation in the value of the interaction between the spins since it depends on their separation. Generally speaking, a minimum Hamiltonian based on the Heisenberg model deals with the atom displacements from their equilibrium positions[20, 27, 28]. This Hamiltonian may consider the interactions between the first neighbors independent of their length so that the exchange interaction depends on the oscillations around the equilibrium position as $J_{ij}(|\mathbf{r}_{ij}^0 + \mathbf{u}_i - \mathbf{u}_j|)$, where \mathbf{r}_{ij}^0 indicates the equilibrium distance between the first neighbors and \mathbf{u}_i (\mathbf{u}_j) corresponds to the displacement vector of each site i (j) from its respective regular position. This trick also takes into account the occurrence of small displacements compared to the equilibrium distance between the atoms, that is, $|\mathbf{u}_i|/|\mathbf{r}_{ij}^0| \ll 1$. This strategy allows us to carry out an expansion of the exchange interaction around the equilibrium position in such a way that, when we ignore the terms of higher orders, we have:

$$(|\mathbf{r}_{ij}^0 + \mathbf{u}_i - \mathbf{u}_j|)J_{ij} = J_{ij}(|\mathbf{r}_{ij}^0|) + \frac{dJ_{ij}}{dr}\bigg|_{r=|\mathbf{r}_{ij}^0|} \mathbf{e}_{ij} \cdot (\mathbf{u}_i - \mathbf{u}_j), \quad (1)$$

where $J_{ij} = J_{ij}(|\mathbf{r}_{ij}^0 + \mathbf{u}_i - \mathbf{u}_j|)$ and $\mathbf{e}_{ij} \equiv \mathbf{r}_{ij}^0/|\mathbf{r}_{ij}^0|$ is the vector that connects two neighboring sites i and j in their respective equilibrium positions. Also, the first term of Eq. (1) is a constant that depends only on the equilibrium distances and therefore represents an undisturbed exchange interaction. The second one allows for the distortions of the crystalline lattice promoted by the negligible displacements of the atoms. More importantly, we can use this exchange interaction also for systems that contain Ising-like spins, obtaining a Hamiltonian of the

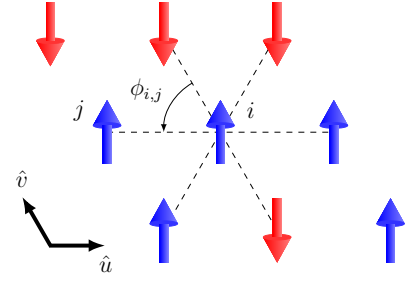


FIG. 1. Representation of a configuration in the triangular lattice. The dotted lines indicate the interactions between the first neighbors of the site i . Taking the direction given by the vector \hat{v} as the main axis, the angle $\phi_{i,j} = 60^\circ$ is represented in the figure.

type

$$\mathcal{H} = - \sum_{\langle i,j \rangle} J_{ij} \sigma_i \sigma_j, \quad (2)$$

where σ_i is the spin variable that can assume ± 1 .

In this work, we adjusted this approach considering that displacements can only occur in a preferred direction, called the main axis. Furthermore, we fix the principal axis along one of the directions connecting two neighboring sites. Then the exchange interaction can be written as

$$J_{ij} = J + J_a \cos(n\phi_{ij}), \quad (3)$$

where J_a is a phenomenological parameter that is related to the influence of phonons on spin interactions and ϕ_{ij} is the angle formed from an orientation taken on the main axis and the line that joins the spins neighbors i and j . Since we chose to position the main axis in the direction of one of the possible interactions, we can choose the main axis in the direction of the vector \hat{v} as shown in Fig.1. In this sense, when we adopt a triangular lattice, we observe that the angles formed between the main axis and the interactions between neighboring spins are multiples of 60° .

Another important aspect of our proposal is the role of the variable n that is responsible for ensuring the isotropy of bonds between two neighboring spins. Basically, on the triangular lattice, we can separate the possible values for n into two cases: (i) - n is a multiple of 6, and (ii) - n is not a multiple of 6. For case (i) we will have $J_{ij} = J + J_a$ for all connections, so that, for $J_a > 0$ Eq. (2) will represent the ferromagnetic triangular Ising model with reinforced interactions, whereas with $J_a < 0$ and $|J_a| > J$, we will have the antiferromagnetic triangular Ising model which, in particular, belongs to a frustrated systems class [29]. For case (ii) we will have $J_{ij} = J + J_a$ for connections in the direction of the main axis and $J_{ij} = J - J_a/2$ for the other connections. In this work, we will adopt case (ii) using the value $n = 2$. Given the main interest in investigating the effects caused by

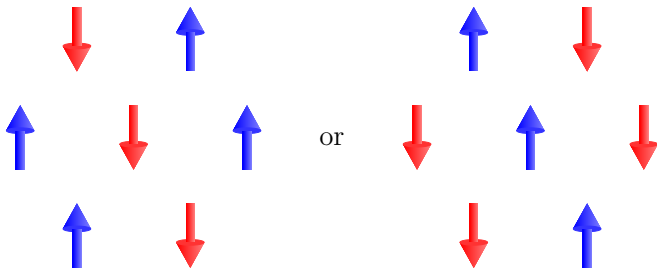


FIG. 2. Ground states for $J = 1.0$ and $J_a = 4.0$. In the direction of the main axis, the spins have a ferromagnetic order. Such configurations will be called Stripes.

the vibration of atoms in the lattice, we consider $J = 1$. Allied to this, when $J_a = 0$, the system represents the standard 2D triangular Ising model. Otherwise, the interaction energy of a spin with its first neighbors is given by

$$\frac{\mathcal{H}_{i,j}}{\sigma_{i,j}} = - (1 + J_a)(\sigma_{i,j-1} + \sigma_{i,j+1}) - (1 - \frac{J_a}{2})(\sigma_{i-1,j-1} + \sigma_{i-1,j} + \sigma_{i+1,j+1} + \sigma_{i+1,j}), \quad (4)$$

where the index $i(j)$ is associated with translations in the $\hat{u}(\hat{v})$ direction. In this equation, the first term represents the interactions on the main axis, while the second term refers to the interactions outside this axis. Based on the exposition of Eq.(4), we can verify that for $J_a > 0$ the interactions outside the \hat{v} axis are null when $J_a = 2$, making the system analogue to the one-dimensional case. In this case, there is a comparability with the Ising 1D model for $J = 3$. For $J_a > 2$ the ground state changes from ferromagnetic to a one formed by stripes (*ST*), which are ferromagnetically organized lines as shown in Fig 2. This happens because the ferromagnetic interaction energy located on the \hat{v} axis is much greater than the interaction energy of the spins outside this axis. An example that supports the representation of this behavior occurs when we consider $J_a = 4$.

III. COMPUTATIONAL DETAILS

We will use entropic simulations to obtain the thermodynamic properties of the system to characterize the phase transitions of the model. This tool proved to be effective in the study of critical phenomena due to its ability to obtain thermodynamic quantities at any temperature. Its use became more effective after the publication of the Wang-Landau algorithm [30, 31], whereby leveling the energy histogram, followed at each simulation step, it is possible to obtain a good estimate for the density of states $g(E)$. This methodology allows estimating any thermodynamic quantity X through the canonical mean

$$\langle X \rangle = \frac{\sum_E X_E g(E) e^{-\beta E}}{\sum_E g(E) e^{-\beta E}}, \quad (5)$$

where X_E represents the microcanonical average that was accumulated during the simulation. Since the density of states corresponds to a very large number, it is convenient to adhere to the simulation with the logarithm of the density of states, $S(E) = \ln g(E)$, identified as the microcanonical entropy. At the beginning of the simulation, we assume $S(E) = 0$ and choose the lowest energy configuration as the starting point. A new configuration is obtained by changing the spin state of a random site, whose acceptance probability is given by

$$P(E_\mu \rightarrow E_\nu) = \min(e^{S(E_\mu) - S(E_\nu)}, 1). \quad (6)$$

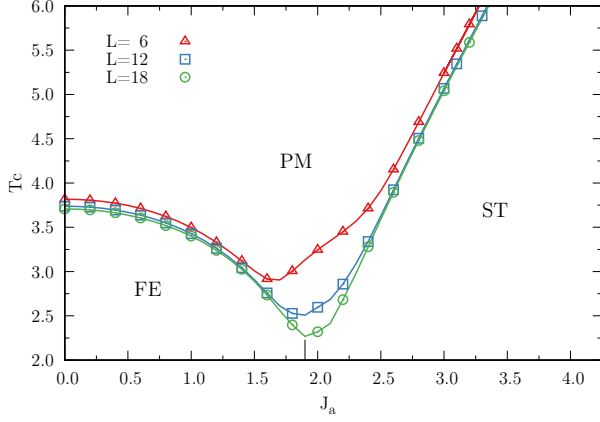
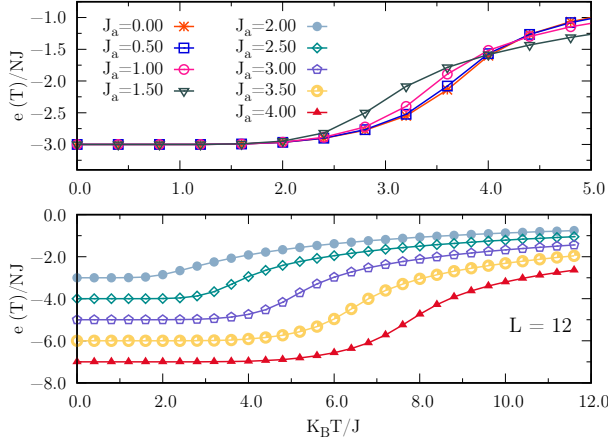
At each change attempt, we update the energy histogram and the logarithm of the density of states $H(E_\nu) \rightarrow H(E_\nu) + 1$ and $S(E_\nu) \rightarrow S(E_\nu) + F_i$, respectively. $F_i = \ln f_i$ and f_i the modification factor that initially corresponds to $f_0 \equiv e = 2.71828 \dots$ [30]. Then, at each flatness condition met, we update f_i based on the criterion $f_{i+1} = \sqrt{f_i}$ and then the histogram is reset. Going beyond what is proposed in the original article by Wang-Landau, in this process we accumulate the microcanonical averages from f_7 [32] where the histogram is expected to be flat. We end the simulation at a f_{final} that ensures the accumulated canonical mean throughout the simulation, whereas in this work we end at f_{15} which is also recognized as the sixteenth level of Wang-Landau. In addition, a two-dimensional approach to the density of states $g(E_1, E_2)$ can be used, allowing estimation of thermodynamic quantities for any values of the energy parameters of E_1 and E_2 [33]. Its use allows one to obtain a sketch of the phase diagram of the system. However, there is a significant increase in computational time, using only small lattice sizes. The simulations protocol is kept unchanged, the only changes are that $g(E) \rightarrow g(E_1, E_2)$ and $H(E) \rightarrow H(E_1, E_2)$. The canonical mean of a quantity X is given by

$$\langle X \rangle = \frac{\sum_{E_1, E_2} X_{E_1, E_2} g(E_1, E_2) e^{-\beta E}}{\sum_{E_1, E_2} g(E_1, E_2) e^{-\beta E}}, \quad (7)$$

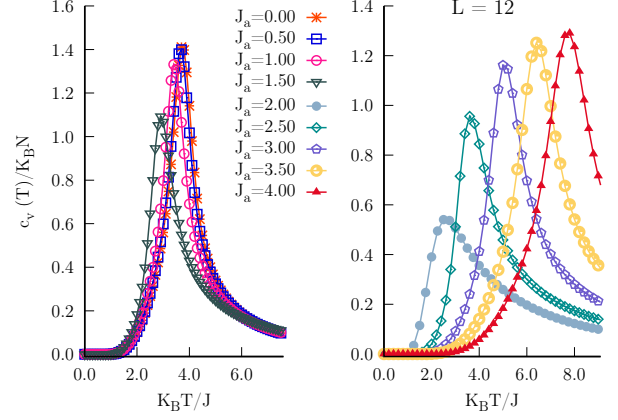
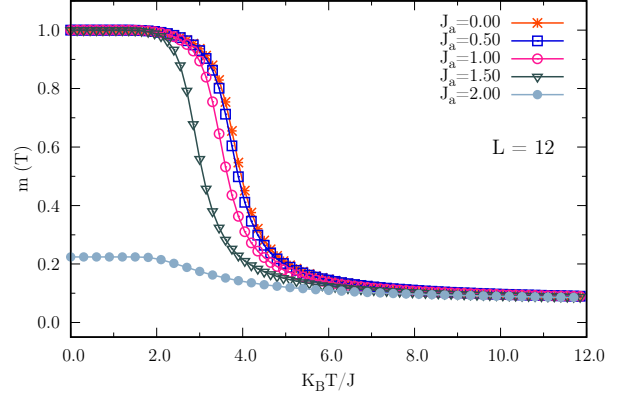
where $E = JE_1 + J_a E_2$.

IV. RESULTS

To establish a more in-depth description of the behavior of the model, we initially sought to calculate essential thermodynamic quantities such as energy, specific heat, magnetization, susceptibility and other properties through the simulation method linked to the calculation of the density of states $g(E, M)$. The two-dimensional approach to the density of states allowed us to explore more quickly the influence provoked in the lattice of spins established by the different values assumed by J_a . However, despite this gain, we are limited to smaller lattice sizes corresponding to $L = 6$, $L = 12$ and $L = 18$. To guide the study of this model from the perspective of $J_a > 0$, we started our approach at this first moment,

FIG. 3. Phase diagram for $J_a \geq 0$.FIG. 4. Energy as a function of temperature for several values of J_a .

seeking to highlight the phase diagram of the model (Fig.3). Its construction was established from the extraction of the critical temperature corresponding to the maximum of the specific heat linked to each value attributed to J_a that belongs to the interval of interest. In addition, we also identified that the data shown in Fig.3 has a high degree of similarity with works that, despite having a more complex Hamiltonian, address the same degrees of freedom of spins considered here[34]. In this last reference, for example, it was also observed in the phase diagram of a ferromagnetic system that the coupling with the lattice decreases the transition temperature of the magnetic system before a certain critical coupling value and increases the transition temperature after this value. This fact is clearly described here as observed in Fig.3. Another aspect that deserves attention regarding this graph is when the model behaves similarly to a one-dimensional system, as in $J_a = 2.0$. And although this characteristic was already predicted by the equation Eq.(4), in this initial stage the simulations were able to show strong evidence of the existence of a critical temperature associated with this point, as observed

FIG. 5. Specific heat as a function of temperature for various values of J_a .FIG. 6. Magnetization as a function of temperature for several values of J_a .

in Fig.3 and Fig.5. Given this, it is also worth mentioning that the confirmation of this characteristic is already supported by results from recently published works[35].

Other points that improve the understanding of the model are exposed when we evaluate the thermodynamic properties together with the phase diagram. In Fig.4 we obtain the mean energy per spin so that the value corresponding to the ground state for $0 \leq J_a \leq 2$ is equivalent to $-3J$, whose representation is associated with a ferromagnetic phase in that same interval (a fact already supported by the analytical evaluation of the model). Still in the region of low temperatures when we observe the values of $J_a > 2$, a new symmetry appears in the ground state identified as the *stripes* phase (St) which in this case is composed of vertical lines of spins that align in an ordering *up* and *down* alternately, which is also shown according to the analytical exposition. From the graph of the specific heat observed in Fig.5 we verify that with $J_a = 0.00$ (pure Ising model in the triangular lattice) a peak appears corresponding to the critical temperature of the ferro-paramagnetic phase transition, whose analyt-

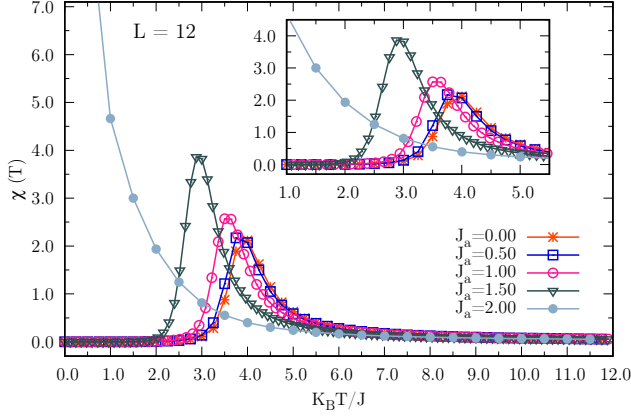


FIG. 7. Magnetic susceptibility as a function of temperature for several values of J_a .

ical value is $k_B T_c/J \approx 3.65364$. And although this value was extracted from a small lattice, it is reasonable as observed in other works [36] to provide us with even more confidence regarding the adequacy of pure Ising model.

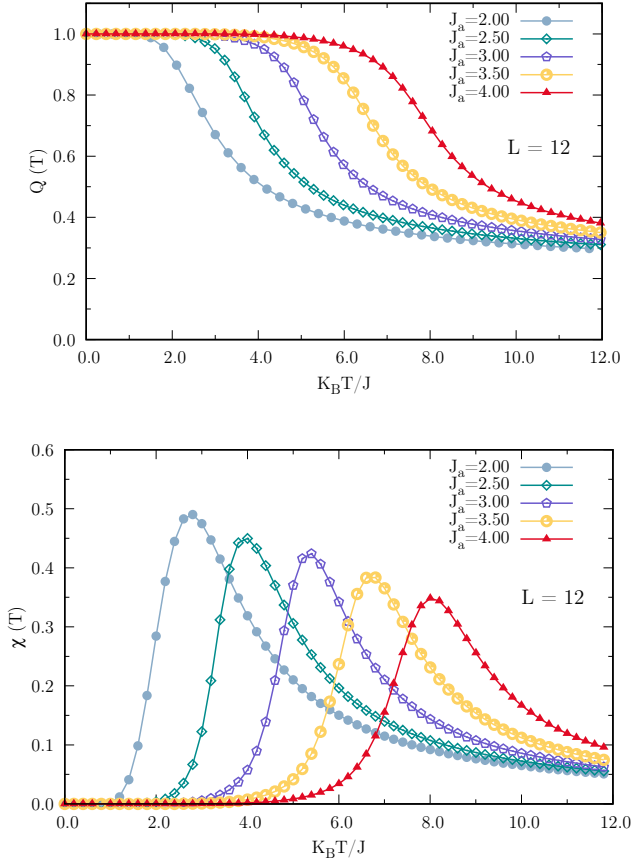


FIG. 8. Order parameter and susceptibility as a function of temperature for several values of $J_a \geq 2$.

Along the same lines, it is also possible to observe a dual behavior of the specific heat peak, whose maximum

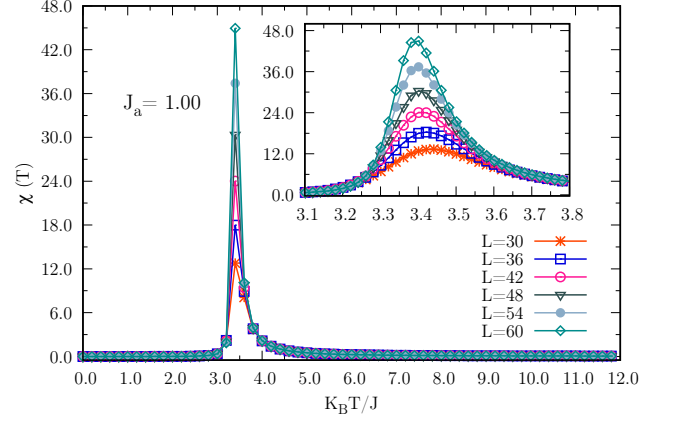


FIG. 9. Susceptibility as a function of temperature to $J_a = 1.0$

undergoes a shift to the left in the range of $0 \leq J_a \leq 2$ indicating a progressively lower ferromagnetic transition temperature and in the range of $2 < J_a \leq 4$ we observe the opposite behavior for the maximum of the specific heat that now undergoes a translation to the right and reaches increasingly higher transition temperatures for each value assigned to the J_a parameter.

The abrupt distinction in behavior reinforces the presence of a new ordered state at low temperatures that appears with increasingly lower energies as shown in Fig.4 for the interval $2 < J_a \leq 4$ that need to reach higher energy levels to break the ordering of the *stripes* phase and evolve into the paramagnetic phase. Still from the perspective of the same lattice size, we can observe the magnetization (Fig.6) and susceptibility (Fig.7) behavior of the system for various values of J_a . In this context, we can observe that the magnetization of the system starts at 1.0, reinforcing a classic behavior of a ferromagnetic system, and suffers a transition temperature difference for each value of $J_a < 2.0$. The correspondence of these transition points is also observed in the maxima presented by the susceptibility for this same range of J_a values. In a completely different direction, we observe an atypical behavior in both graphs for $J_a = 2.0$, which was already expected given the fact that this value of J_a signals the threshold of the two phases as it is pronounced in the phase diagram. This feature, which was also predicted by the analytical route of the model, forced the system to have one-dimensional dynamics in the face of the established decoupled columns.

From this point on, the *stripes* phase emerges. To explore this region in more depth, we need to present a new order parameter that is capable of meeting this expectation. This parameter was established as

$$Q = \sum_{i=1}^L \left| \sum_{j=1}^L \sigma_{ij} \right|, \quad (8)$$

where Q corresponds to the final result of the sum of the

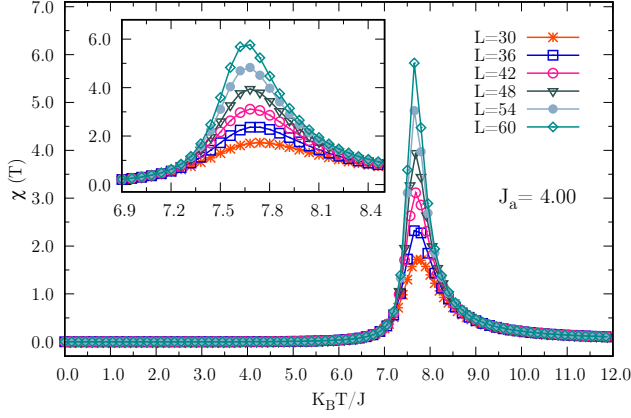


FIG. 10. Susceptibility as a function of temperature for $J_a = 4.0$

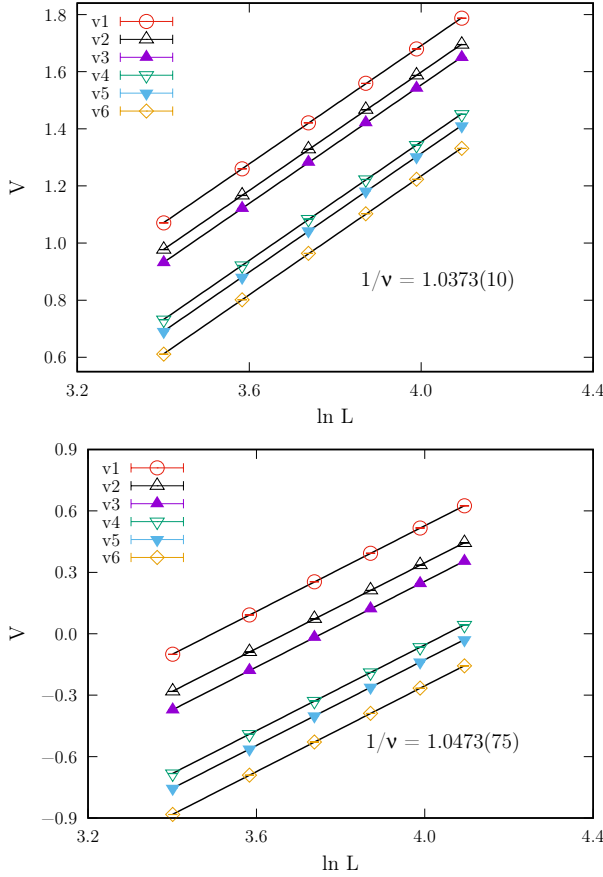


FIG. 11. Graphs of $1/\nu$ for $J_a = 1.0$ and $J_a = 4.0$ respectively.

modules obtained from each sum of the spins arranged vertically. Using this artifice, we obtain the characteristic behavior of an order and susceptibility parameter for $J_a = 2.0$ and for values greater than this that fall within the *stripes* phase, as shown in figure Fig.8. The need to better understand the scalability of the system at points whose regions are well defined together with

the guarantee of the validity of the parameter Q raises the confidence level to investigate the *stripes* phase and the ferromagnetic phase for lattice sizes even bigger. To achieve this goal we performed the simulations with $g(E)$ instead of $g(E, M)$ for different lattice sizes ranging from 30 to 60 as can be seen in the figures Fig.9 and Fig.10. In both graphs, it is possible to see the existence of transition signals for each lattice size and a scaling law that is associated with the respective sizes. These results reinforce the feasibility of exploring the behavior of the system for $J_a = 1.0$ (representing the ferromagnetic phase) and $J_a = 4.0$ (representing the *stripes* phase).

For this, we use the finite size scaling theory so that the results can be projected to an infinite size. According to this theory we obtain a universal form for the molar Helmholtz free energy corresponding to the equation

$$f(t, H; L) = L^{-d} Y(atL^{1/\nu}, bHL^{\Delta/\nu}), \quad (9)$$

this expression identifies the reduced temperature t which is equivalent to $(T - T_c)/T_c$, the external field H , the metric factors a and b , the spatial dimension of the system d , the static critical exponents ν and Δ and the linear dimension of the system L . From this, it is possible to extract system information equivalent to magnetization, susceptibility and specific heat through the equation (9) [37, 38]. At $H = 0$ such features follow the following scaling laws

$$m \approx L^{-\beta/\nu} m'(tL^{1/\nu}), \quad (10)$$

$$\chi \approx L^{\gamma/\nu} \chi'(tL^{1/\nu}), \quad (11)$$

$$c \approx c_\infty + L^{\alpha/\nu} c'(tL^{1/\nu}). \quad (12)$$

In the critical region ($t = 0$), we identify the universal scaling functions m' , χ' and c' as constants and the static critical exponents β , γ and α that make up the base responsible for identifying the universality class that the system fits [39]. These exponents obey the scale and hyperscale relationships recognized as the Fisher, Rushbrooke, Widom, and Josephson [40] relationships. Despite the usefulness of these relations, it is observed a certain difficulty in eliminating the dependence that each thermodynamic property of interest has on the exponent ν . Thus, to obtain it in isolation, we use the equation

$$V_j \approx (1/\nu) \ln L + V'_j(tL^{1/\nu}). \quad (13)$$

In this equation we have $j = 1, \dots, 6$, where V'_j are constants independent of the size of the system that represent thermodynamic quantities extracted from the logarithm of the derivative of magnetization. At the critical temperature, (T_c) these functions converge to their corresponding value in the infinite lattice so that when we perform a linear adjustment of the graph referring to $V_j \times L$ we can calculate $1/\nu$. Having found the exponent ν

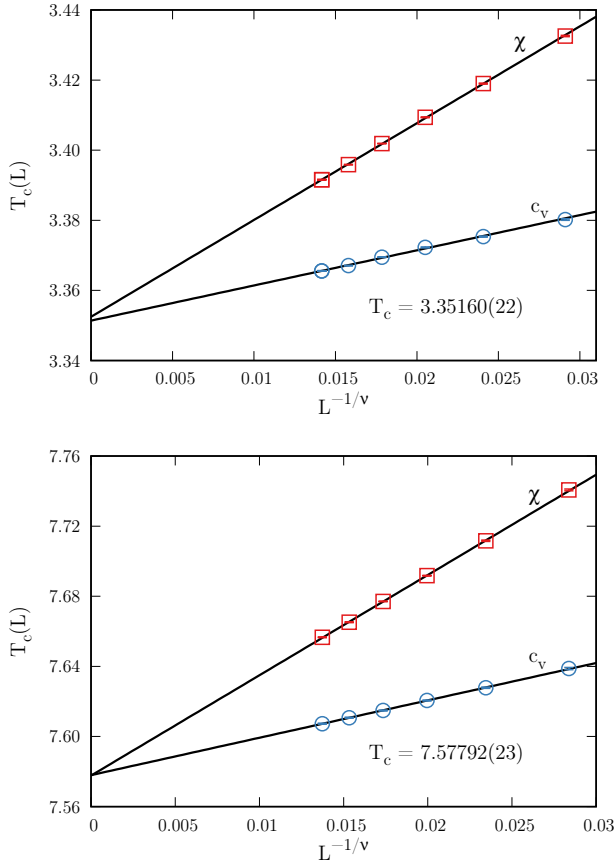


FIG. 12. Graphs of T_c for $J_a = 1.0$ and $J_a = 4.0$ respectively.

and the specific heat and susceptibility maxima, we can estimate the critical temperature using the equation

$$T_c(L) \approx T_c + a_q L^{-1/\nu}, \quad (14)$$

where a_q is identified as a constant. Following all the steps of this theory we managed to obtain the first critical exponent of interest as displayed by the graph Fig.11.

In this graph, when we take into account the average standard deviation $\Delta\nu = \Delta(1/\nu)/(1/\nu)^2$ that is associated with this exponent we find for $J_a = 1.0$ the value of $\nu = 0.96404(93)$ and for $J_a = 4.0$ the value of $\nu = 0.9548(68)$.

From these data we extract the critical temperature as shown in the graph Fig.12, in this graph the transition temperature from the ferromagnetic phase ($J_a = 1.0$) to the paramagnetic phase is equivalent to $T_c = 3.35160(22)$, on the other hand, the transition temperature from the stripes phase ($J_a = 4.0$) to the paramagnetic phase presents a transition temperature corresponding to $T_c = 7.57792(23)$.

In the graph Fig.13 we obtain for $J_a = 1.0$ the result $\gamma/\nu = 1.7622(15)$ and for $J_a = 4.0$ the result $\gamma/\nu = 1.7520(10)$ and the associated error being γ equivalent to $\Delta\gamma = \Delta\nu(\gamma/\nu) + \nu\Delta(\gamma/\nu)$ it turns out that for $J_a = 1.0$ we have $\gamma = 1.6988(31)$ and for $J_a = 4.0$ we obtain the

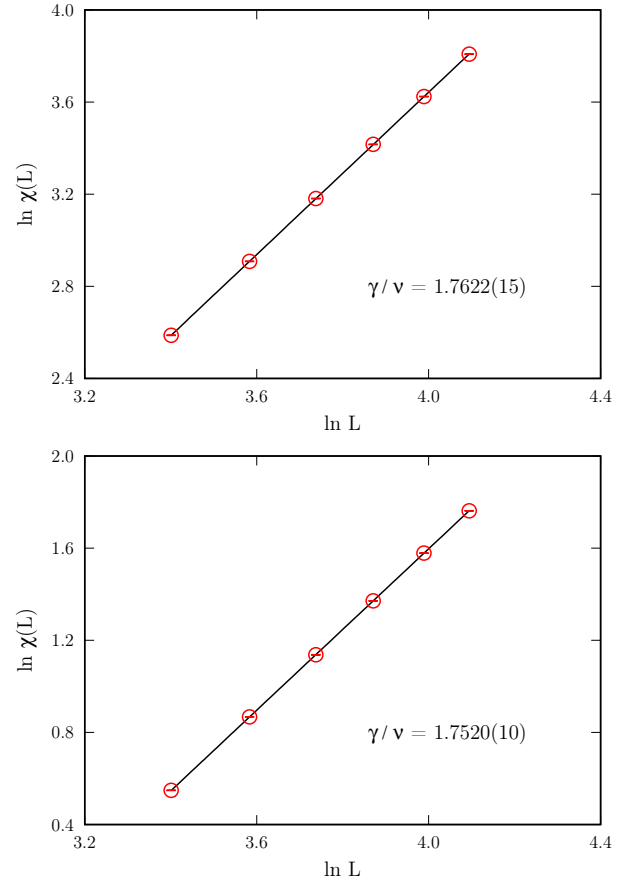


FIG. 13. Graph of γ/ν for $J_a = 1.0$ and $J_a = 4.0$ respectively.

exponent $\gamma = 1.673(13)$

To calculate the last critical exponent we used the results of the graph Fig.14 where for $J_a = 1.0$ we have $\beta/\nu = 0.1327(12)$ and for $J_a = 4.0$ we obtain $\beta/\nu = 0.1280(19)$, knowing that the error associated with β is $\Delta\beta = \Delta\nu(\beta/\nu) + \nu\Delta(\beta/\nu)$ we have $\beta = 0.1279(13)$ for $J_a = 1.0$ and $\beta = 0.1222(34)$ for $J_a = 4.0$.

This entire set of results just presented for the critical exponents γ/ν and β/ν for the system with $J_a = 1.0$ and with $J_a = 4.0$ also provides us with strong evidence that the model has the same universality class as the two-dimensional Ising model that has exponents $\gamma/\nu = 7/4 = 1.75$ and $\beta/\nu = 1/8 = 0.125$ as it is also adopted as a reference parameter in other works [36, 41]. Furthermore, given the strong evidence exposed so far, it is also possible to infer that the respective transitions from both the ferromagnetic and *Stripes* phases to the paramagnetic phase fall within transitions characterized as second order.

V. CONCLUSION

In this work, we propose a different and physically more adequate way to describe the dynamics of Ising-

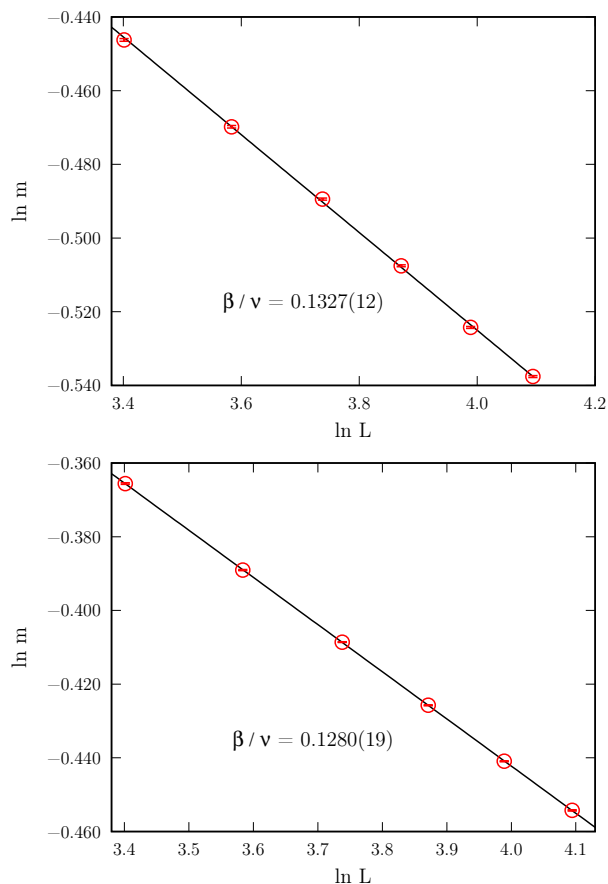


FIG. 14. Graph of β/ν for $J_a = 1.0$ and $J_a = 4.0$ respectively.

like magnetic spins located under a crystalline lattice. The main focus of this proposal was to evaluate how the lattice vibration under a preferential direction interferes with the spin interaction dynamics and what is its reper-

cussion on the phase transition temperature for each lattice coupling factor considered. Based on this, we established a Hamiltonian that, as a result of this study, proved capable of meeting this purpose, presenting strong results from classical thermodynamic properties and robust techniques such as finite-size scaling that proved to be useful in determining the universality class of the system.

Another merit worth highlighting concerns the additional interaction adopted in this work whose composition considers the symmetry of the chosen lattice. The presence of this artifact in the Hamiltonian managed to promote a rotational anisotropy that altered the interaction dynamics of the spins favoring the interactions taken on a preferential direction that coincides with the direction of propagation of the phonons. As a consequence of this process, the adoption of the proposed Hamiltonian for the triangular lattice demonstrated that up to $J_a = 2.0$ the coupling with the lattice favors the ferro-paramagnetic phase transition. On the other hand, after this factor, the coupling with the lattice disfavors the *Stripes* - paramagnetic transition. The mathematical representation of the model also allowed us to obtain some analytical developments that served to clarify the behavior of the system in its singularity and to guide this entire study developed throughout the simulations.

In this sense, despite the simplicity of this approach, the impacts are extremely relevant. Because when we explore a single type of lattice considering only $J_a \geq 0.0$ the system can also represent similar behaviors that are linked to more complex models, in addition to the two-dimensional Ising model in the triangular lattice (when $J_a = 0.0$) and the one-dimensional Ising model (when $J_a = 2.0$). In this way, it is to be expected that by expanding the range of investigation routes of this proposal, either by changing the degrees of freedom of the spins or the type of lattice, we will be able to achieve even more surprising results.

-
- [1] J. Gregg, I. Petej, E. Jouguet, and C. Dennis, *Journal of Physics D: Applied Physics* **35**, R121 (2002).
 - [2] E. C. Ahn, *npj 2D Materials and Applications* **4**, 1 (2020).
 - [3] W. Andreoni and S. Yip, *Handbook of materials modeling: methods: theory and modeling* (Springer, 2020).
 - [4] B. A. Cipra, *The American Mathematical Monthly* **94**, 937 (1987).
 - [5] A. S. T. Pires, *Theoretical tools for spin models in magnetic systems* (IOP Publishing, 2021).
 - [6] F.-Y. Wu, *Reviews of modern physics* **54**, 235 (1982).
 - [7] K. Choo, T. Neupert, and G. Carleo, *Phys. Rev. B* **100**, 125124 (2019).
 - [8] H. Diep *et al.*, *Frustrated spin systems* (World Scientific, 2013).
 - [9] R. F. Evans, W. J. Fan, P. Chureemart, T. A. Ostler, M. O. Ellis, and R. W. Chantrell, *Journal of Physics: Condensed Matter* **26**, 103202 (2014).
 - [10] J. Oitmaa and M. N. Barber, *Journal of Physics C: Solid State Physics* **8**, 3653 (1975).
 - [11] R. J. Bursill, R. H. McKenzie, and C. J. Hamer, *Physical review letters* **83**, 408 (1999).
 - [12] J. Yin, M. Eisenbach, D. M. Nicholson, and A. Rusanu, *Journal of Applied Physics* **113**, 17E112 (2013).
 - [13] J. Li, J. Feng, P. Wang, E. Kan, and H. Xiang, *Science China Physics, Mechanics & Astronomy* **64**, 1 (2021).
 - [14] L. Casto, A. Clune, M. Yokosuk, J. Musfeldt, T. Williams, H. Zhuang, M.-W. Lin, K. Xiao, R. Henig, B. Sales, *et al.*, *APL materials* **3**, 041515 (2015).
 - [15] H.-R. Fuh, C.-R. Chang, Y.-K. Wang, R. F. Evans, R. W. Chantrell, and H.-T. Jeng, *Scientific reports* **6**, 32625 (2016).
 - [16] T. Egami, B. Fine, D. Parshall, A. Subedi, and D. Singh, *Advances in Condensed Matter Physics* **2010** (2010).
 - [17] T. Birol and C. J. Fennie, *Physical Review B* **88**, 094103 (2013).

- [18] J. H. Lee, L. Fang, E. Vlahos, X. Ke, Y. W. Jung, L. F. Kourkoutis, J.-W. Kim, P. J. Ryan, T. Heeg, M. Roeckherath, *et al.*, *Nature* **466**, 954 (2010).
- [19] B. Sadhukhan, A. Bergman, Y. O. Kvashnin, J. Hellsvik, and A. Delin, *Physical Review B* **105**, 104418 (2022).
- [20] K. Aoyama, M. Gen, and H. Kawamura, *Physical Review B* **104**, 184411 (2021).
- [21] O. Tchernyshyov and G.-W. Chern, in *Introduction to Frustrated Magnetism: Materials, Experiments, Theory* (Springer, 2010) pp. 269–291.
- [22] D. L. Bergman, R. Shindou, G. A. Fiete, and L. Balents, *Physical Review B* **74**, 134409 (2006).
- [23] M. A. McGuire, G. Clark, K. Santosh, W. M. Chance, G. E. Jellison Jr, V. R. Cooper, X. Xu, and B. C. Sales, *Physical Review Materials* **1**, 014001 (2017).
- [24] P.-W. Ma, C. Woo, and S. Dudarev, *Physical review B* **78**, 024434 (2008).
- [25] J. Choe, D. Lujan, M. Rodriguez-Vega, Z. Ye, A. Leonardo, J. Quan, T. N. Nunley, L.-J. Chang, S.-F. Lee, J. Yan, *et al.*, *Nano Letters* **21**, 6139 (2021).
- [26] S. Mankovsky, S. Polesya, H. Lange, M. Weißenhofer, U. Nowak, and H. Ebert, *Physical Review Letters* **129**, 067202 (2022).
- [27] C. Jia, J. H. Nam, J. S. Kim, and J. H. Han, *Physical Review B* **71**, 212406 (2005).
- [28] F. Wang and A. Vishwanath, *Physical Review Letters* **100**, 077201 (2008).
- [29] R. Moessner and S. L. Sondhi, *Physical Review B* **63**, 224401 (2001).
- [30] D. Landau, S.-H. Tsai, and M. Exler, *American Journal of Physics* **72**, 1294 (2004).
- [31] F. Wang and D. Landau, *Physical review letters* **86**, 2050 (2001).
- [32] Á. d. A. Caparica and A. G. d. Cunha-Netto, *Physical Review E* **85**, 046702 (2012).
- [33] L. S. Ferreira, L. N. Jorge, C. J. Da Silva, and A. A. Caparica, *Brazilian Journal of Physics* (2021).
- [34] L. Pili and S. A. Grigera, *Physical Review B* **99**, 144421 (2019).
- [35] L. S. Ferreira, L. N. Jorge, C. J. DaSilva, M. A. Neto, and A. Caparica, *arXiv preprint arXiv:1911.05475* (2019).
- [36] E. Vatansever, *Physica A: Statistical Mechanics and its Applications* **511**, 232 (2018).
- [37] H. E. Stanley, *Introduction to Phase Transitions and Critical Phenomena*, first edition ed., *Monographs on Physics* (Oxford University Press, 1971).
- [38] A. Caparica, A. Bunker, and D. Landau, *Physical Review B* **62**, 9458 (2000).
- [39] A. Caparica, S. A. Leão, and C. J. DaSilva, *Physica A: Statistical Mechanics and its Applications* **438**, 447 (2015).
- [40] K. Huang, *Statistical mechanics* (Wiley, 1987).
- [41] A. Caparica, *Physical Review E* **89**, 043301 (2014).